Electric Field Behavior near a Contact Point in the Presence of Volume Conductivity

B. Techaumnat, S. Hamada, T. Takuma

Dept. of Electrical Engineering
Kyoto University, Kyoto, Japan

ABSTRACT

The electric field behavior, in particular the field intensification at a contact point, is very important in complex dielectric systems with gaseous or vacuum insulation. The paper describes the electric field behavior at and near a contact point in various arrangements with a zero contact angle when volume conductivity is present in the solid dielectric. Contact conditions are separated into line, point, and surface contact. The effect of volume conductivity is investigated analytically, and numerically by using the boundary element method. The electric field behavior near a contact point principally depends on the absolute value of complex relative permittivity, and volume conductivity usually promotes the field intensification. In the arrangements of point contact or line contact, the position of peak electric field shifts from a contact point when the volume conductivity is higher than a certain value, while in the arrangement of surface contact, the position is usually more or less remote from the contact point, whether volume conductivity is present or not.

1 INTRODUCTION

VARIOUS insulation systems are now in extensive use, such as gaseous, liquid, solid, and vacuum. In all these systems, except for solid insulation, a solid dielectric is required to provide support and separation of a stressed conductor. The electric field behavior near a contact point between solid dielectric surface and an electrode (triple-junction point) is very complicated, and often is much higher when compared with the field without solid dielectric [1, 2]. It depends heavily on contact conditions and material properties of the media.

The electric field behavior near a contact point has a strong effect on insulation design, particularly where a gaseous dielectric is involved. This is because the dielectric strength of gaseous dielectrics substantially decreases when partial discharge (PD) takes place due to the field intensification inside the system. In practice, solid dielectric has more or less conductivity which may affect the field behavior. Although the field behavior has already been studied in detail in various contact conditions, the effect of conductivity has not been fully analyzed until now. When conductivity is involved, analytical solutions exist only for some limited cases of the triple-junction problems. Although numerical field calculations have been applied to a few problems, the understanding of the effect of conductivity is far from satisfactory.

The triple-junction problems may be separated according to their contact angle α into the following three categories:

1. α=90° (Figure 1(a))
2. 0<α<90° or 90<α<180° (Figure 1(b))
3. α=0° (Figure 1(c))

In the first category, although the presence of a solid dielectric may alter the electric field distribution without the solid dielectric, field singularity does not take place.

The second category of arrangements with a contact angle 0<α<90° or 90<α<180°, has been studied in the 2-dimensional case for both the effect of permittivity [3, 4] and the effect of conductivity [5] by a group including one of the authors. The electric field near a triple-junction (contact) point approaches an infinite or zero value when the media are perfect dielectrics without any conductivity, depending on the contact angle and the permittivities of the media. They also report that the presence of volume conductivity usually promotes the field singularity near the contact point.

The last category, the triple junction problem of a zero-angle contact condition, has been investigated only for the effect of permittivity in some typical arrangements [5, 6]. Although field intensification takes place near a contact point, the electric field at the contact point is not singular. The effect of the conductivity has not been investigated yet for this contact condition.

In this paper, we analyze the effect of volume conductivity in various conditions. To make clear the general characteristics of the field

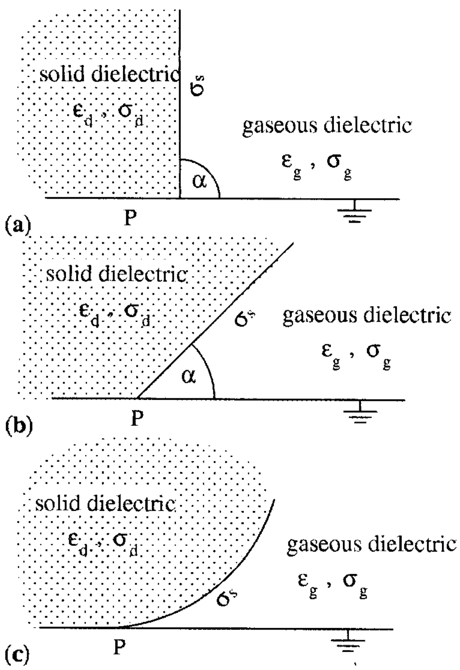

Figure 1. Contact angle at a triple junction. (a) α=90°, (b) 0<α<90°, (c) α=0°.

distribution near a zero-angle contact point, it is to be noted here that the contact conditions should be also divided into line contact (2-dimensional case), point contact (axisymmetrical case), and surface contact. We have applied the boundary element method with second order curved elements as a numerical calculation method in the analysis.

2 CALCULATION METHODS

2.1 THE BOUNDARY ELEMENT METHOD

Numerical field calculation methods can be divided basically into two main groups. The first one is the domain subdivision method such as the finite difference method and the finite element method, and the second one is the boundary subdivision method such as the charge simulation method and the boundary element method. The former is a more general method, having flexibility so that it can be applied to any problem, including nonlinear characteristics of media. The domain under consideration is discretized into a number of cells. The solution of the problem, usually potential, is approximated over the region and then determined so as to satisfy the governing equations. The electric field usually is calculated as a derivative of the approximated potential.

In the latter method, usually, only boundaries of the domain are subdivided (although domain subdivision is required in the case of internally charged insulators). Dimension of the final matrix is smaller than the one in a corresponding domain subdivision method, but the matrix is not usually sparse and needs more time to be solved. However, boundary subdivision methods are generally more accurate in calculating electric field. In this paper, we have used the boundary element method (BEM), one of the boundary subdivision methods, to calculate the electric field in all arrangements.

In the BEM, the normal component of electric field and the potential on all the boundary nodes are determined first. Then, the potential ϕ at any point p in the region can be expressed as

$$C\phi(p) = \int_{\Gamma} E_n w \, d\Gamma + \int_{\Gamma} \phi \frac{\partial w}{\partial n} \, d\Gamma \tag{1}$$

where Γ is the boundary of the region, E_n the normal electric field component on the boundary, C a constant that depends on the position of p, w is the fundamental solution, and $\frac{\partial w}{\partial n}$ is its normal derivative on the boundary.

The fundamental solution w is defined separately for 2-dimensional and axisymmetrical field analysis [8, 9]. In a twodimensional field, for example, $w = (1/2\pi)\ln(1/r)$ where r is the distance between p and the boundary point under consideration.

The BEM can be applied to an inhomogeneous domain by subdividing the domain into regions of a homogeneous medium. The BEM then is applied to each region. The values between two adjacent regions, region 1 and 2, are related on the boundary surface by

$$\phi_1 = \phi_2 \tag{2}$$

$$(\sigma_1 + i\omega\varepsilon_1)E_{n1} = (\sigma_2 + i\omega\varepsilon_2)E_{n2} \tag{3}$$

where σ and ε are the conductivity and permittivity of each region, E_n the normal component of electric field, and ω is the angular velocity.

Equations (1), (2), and (3) are the main equations in the BEM code utilized to calculate electric field distribution in this paper.

2.2 CALCULATION PROCEDURES

Electric fields in arrangements with a zero-angle contact condition tend to rise steeply near a contact point. Reference [7] gives an analytical solution for the arrangement of Figure 2(a) (shown later) in a 2-dimensional field. The analytical solution is obtained by placing an infinite series of line dipoles at a distance R_0/n above the ground plane and at a distance R_0 below the ground plane where $n = 1, 2, 3, \ldots$. The line dipole magnitude in the series decreases at the rate of $(\varepsilon_d - 1)/(\varepsilon_d + 1)$. Obviously, when the relative permittivity ε_d of the solid dielectric is $\gg 1$, the decrease of the magnitude of the line dipoles is very slow. As a result, the dipoles are very densely distributed, resulting in high magnitude just above the ground plane and rapid change of electric field near the contact point.

In order to achieve correct calculation for arrangements with such field behavior, we have had to implement the BEM with high accuracy techniques. The accuracy of the BEM is determined mainly by element quadratures. Distance between boundary surfaces becomes very small near a contact point in these arrangements, thus causing the element quadratures to be quasi-singular.

The log-$L1$ transformation method [10–12] has been adopted here to evaluate quasi-singular quadratures involved in the BEM. Using the method, we have reduced an error of the quadratures to $<10^{-8}$%, even in the case where the distance between an integrated element and a calculation point is $\sim 0.001\times$ the element size.

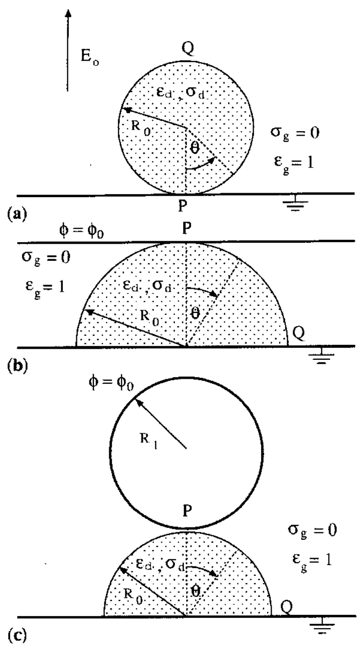

Figure 2. Line or point contact with α=0°. (a) Arrangement 2(a), (b) Arrangement 2(b), (c) Arrangement 2(c).

3 CALCULATION ARRANGEMENTS

We have analyzed the field behavior in the four arrangements shown in Figures 2 and 3.

All the arrangements in Figure 2 have been calculated for both the 2-dimensional and axisymmetrical cases. The contact condition is line contact in the 2-dimensional case and point contact in the axisymmetrical case. The ranges of the relative permittivity ε_d and the conductivity σ_d of the solid dielectric are as follows: ε_d=4 to 12 and σ_d=1 to 20 nS/m, with ε_d=2 or 4.

For simplicity, we will refer to these arrangements in this paper as arrangement 2(a), arrangement 2(b), and arrangement 2(c).

Arrangement 2(a) is a cylindrical or spherical dielectric solid (ε_d, σ_d) lying on a ground plane under a uniform field E_0. Arrangement 2(b) is, by symmetry, equivalent in the electric field to an arrangement of a rounded (cylindrical or spherical) dielectric solid lying between two plane electrodes separated by $2R_0$ (with a potential difference of $2\phi_0$). Arrangement 2(c) also is equivalent to that of a rounded dielectric solid lying between, and in contact with, two cylindrical or spherical electrodes above and below. The ratio R_1/R_0 of arrangement 2(c) is set to 1 in this investigation.

To investigate the field behavior in surface contact with a zero-angle contact condition, we have calculated the arrangement shown in Figure 3 for the 2-dimensional case. Radius b of the rounded side has been varied to examine the effect of the profile where the side has an elliptical cross-section. We have performed the calculation for the following cases: $b/a = 0.5,\ 1,\ 2$, ε_d=4 to 12, and σ_d=1 to 20 nS/m, with ε_d=4. We will refer to this arrangement as arrangement 3 hereafter.

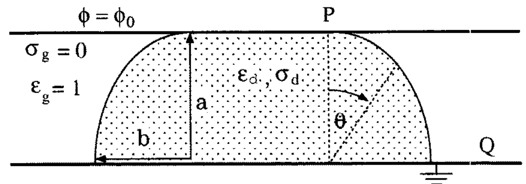

Figure 3. Surface contact with α=0°.

Most insulators used in practice show much lower conductivity in the order of $\lesssim 1$ pS/m. However, conductivity of an insulator increases with increasing temperature and electric stress, often to the order of nS/m. We have chosen the above values of conductivity to make clear the general characteristics on the effect of conductivity. More importantly, the effect of conductivity becomes predominant with decreasing source frequency to dc energization, although the calculation is performed for 50 Hz ac.

For all the arrangements, θ represents an angle starting from the contact point when we describe the field distribution on a rounded dielectric surface.

4 CALCULATION RESULTS

4.1 ANALYTICAL SOLUTION FOR ARRANGEMENT 2(A)

An analytical solution for arrangement 2(a) in the 2-dimensional case of (x, y) can be obtained by placing an infinite series of line dipoles so as to satisfy the boundary conditions on the grounded plane and on the dielectric surface. If we take 1 m as radius R_0 and the center of the cylinder as the origin of the coordinates (x, y), the electric field at any point $\vec{P}(x_0, y_0)$ inside the cylindrical dielectric can be expressed as

$$\vec{E} = a\vec{E}_0 + \sum_{n=1}^{\infty} k_2 M \frac{k_1^{n-1}}{n^2} \frac{(\cos\theta \cdot \vec{a}_r + \sin\theta \cdot \vec{a}_\theta)}{2\pi\varepsilon_0 \varepsilon_d' |\vec{r}|^2} \quad (4)$$

where ε_d' is the complex relative permittivity of the cylindrical dielectric as given below, M the magnitude of the line dipoles, $\vec{Q}_n$ the position vector of the line dipoles, $\vec{a}_r$ and $\vec{a}_\theta$ are unit vectors in the cylindrical polar coordinates, and a, k_1, k_2 are constant numbers.

They are expressed as

$$
\begin{aligned}
\varepsilon_d' &= \varepsilon_d - \mathrm{i}\sigma_d/\omega\varepsilon_0 \\
a &= \frac{2}{\varepsilon_d'+1} \\
k_1 &= \frac{\varepsilon_d'-1}{\varepsilon_d'+1} \\
k_2 &= \frac{2\varepsilon_d'}{\varepsilon_d'+1} \\
M &= 2\pi\varepsilon_0 E_0 k_1 \\
\vec{r} &= \vec{P} - \vec{Q}_n \\
\vec{Q}_n &= (0, \tfrac{-R}{n}) \\
\theta &= \arccos\left(\frac{\vec{r}\cdot\vec{a}_y}{|\vec{r}|}\right) \\
\vec{a}_r &= \frac{\vec{r}}{|\vec{r}|} \\
\vec{a}_\theta &= \vec{a}_r \times \vec{a}_x
\end{aligned} \qquad (5)
$$

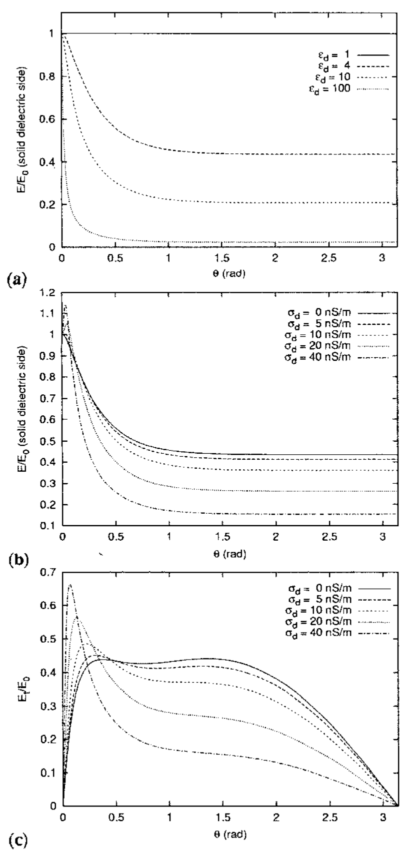

Figure 4. Electric field distribution in arrangement 2(a) for the 2-dimensional case. (a) Effect of permittivity ε_d when σ_d=0, (b) Effect of conductivity σ_d when ε_d=4, (c) Tangential electric field on the solid dielectric surface when ε_d=4.

Figures 4(a), (b), and (c) present the electric field distribution in relation to θ on the solid dielectric side of the dielectric surface. Each electric field on the ordinate is normalized by the uniform field E_0.

Figure 4(a) shows that the electric field strength on the dielectric surface decreases when the permittivity ε_d increases, except at the contact point. The field strength at the contact point is always equal to E_0 and independent of ε_d.

Figure 4(b) shows the effect of volume conductivity σ_d on the electric field distribution when ε_d=4. Surprisingly, the electric field is not always maximal at the contact point. This shift of the peak electric field is noticeable when $\sigma_d \gtrsim 10$ nS/m.

Figure 4(c) presents the distribution of tangential electric field on the surface. The tangential electric field is zero at the contact point due to the zero-angle contact condition. The tangential electric field has a higher peak value and decreases to zero over a smaller region with higher conductivity.

In addition to the analytical solution, a numerical field calculation has been carried out also for arrangement 2(a). We have confirmed that the numerical results show good agreement with the analytical solutions both in the values and positions of the peak electric field. For example, the difference between the analytical solutions and numerical results is ~ 1.9% for the peak electric field and 2.2% for the contact-point electric field when σ_d=20 nS/m.

Results of the numerical calculation are described in the following Sections.

4.2 EFFECT OF σ_D IN ARRANGEMENTS 2

We first concentrate on the electric field at a contact point. Calculation results of the arrangements in Figure 2 are shown in Figure 5.

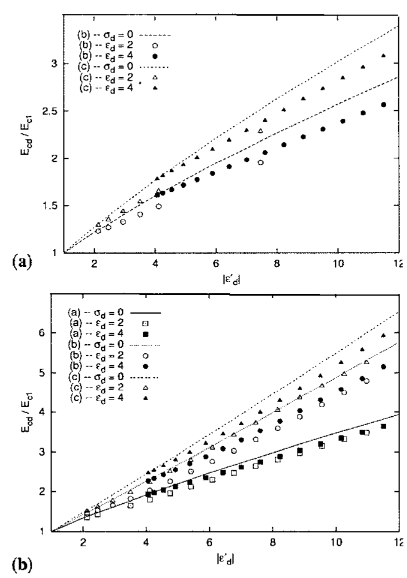

Figure 5. Contact-point electric field in the arrangements of Figure 2. (a) 2-dimensional case, (b) Axisymmetrical case.

Figure 5(a) presents the relation between the contact-point electric field strength on the solid dielectric side E_{cd} and the absolute value of complex relative permittivity ε'_d for arrangement 2(b) and arrangement 2(c) in the 2-dimensional case.

Figure 5(b) presents the corresponding relation for arrangement 2(a), arrangement 2(b), and arrangement 2(c) in the axisymmetrical case. E_{cd} is normalized in the Figures by E_{c1}, the contact-point electric field strength when ε'_d=1. Hollow (rectangular, triangular and circular) points in the Figures indicate E_{cd}/E_{c1} in the case of ε_d=2 while filled points correspond to E_{cd}/E_{c1} in the case of ε_d=4. These calculation results are summarized as follows.

1. The contact-point electric field strength increases with higher ε_d and σ_d in both the 2-dimensional and axisymmetrical cases. This is in contrast to the corresponding contact-point field of arrangement 2(a) in the 2-dimensional case which is constant irrespective of ε_d and σ_d.
2. E_{cd} is approximately decided by $|\varepsilon'_d|$. The same $|\varepsilon'_d|$ makes E_{cd} close to each other among various values of σ_d. However, the larger σ_d gives the lower E_{cd}.
3. When $|\varepsilon'_d|$ is the same, E_{cd} is higher in the axisymmetrical case than in the 2-dimensional one.

An empirical expression has been proposed to approximate E_{cd} for arrangements with a zero-angle contact condition without conductivity as follows [5].

$$E_{cd} = E_{c1} f(\varepsilon_d)$$
$$f(\varepsilon_d) = \frac{\varepsilon_d^k + 1}{2} \qquad (6)$$

where E_{c1} already was defined above, and k is a constant dependent on the arrangement and assumed to lie between 0 and 1.

We have calculated the constant k in Equation (6) for arrangement 2(a), (b), and (c) where $|\varepsilon'_d|$ is substituted for ε_d. When $|\varepsilon'_d| \gtrsim 8$, k takes almost the same value irrespective of whether volume conductivity exists or not.

Figures 6(a) and (b) show the peak electric field strength E_{pg} normalized by the contact-point electric field strength E_{cg} in the gaseous dielectric side where $E_{cg} = |\varepsilon'_d|E_{cd}$. Electric field strength in the gaseous dielectric side is presented here because in practice, electric field in a gaseous dielectric is more important due to the possibility of PD or breakdown. The peak field strength in the gaseous side E_{pg} takes place at a very narrow wedge-like gap. The ratio of peak field strength between both sides of the dielectric surface is not equal to $|\varepsilon'_d|$ because of the tangential component of electric field. As shown in Figures 6(a) and (b), $|\varepsilon'_d| \gtrsim 5.4$, which corresponds to a conductivity of 10 nS/m, leads to E_{pg}>E_{cd}, *i.e.* the shift of the position of E_{pg} from a contact point. The calculation results also agree well with the analytical solution for arrangement 2(a) mentioned in the previous Section. The ratio of E_{pg}/E_{cg} is also higher in the axisymmetrical case than in the 2-dimensional one.

4.3 ARRANGEMENT 3

Arrangement 3 has been calculated for the 2-dimensional case. This is because electric field behavior of this arrangement for the axisymmetrical case is considered very similar near a contact point to that for the 2-dimensional case.

Electric field distributions in the solid dielectric side of the arrangement are presented in Figure 7 for three values of b/a.

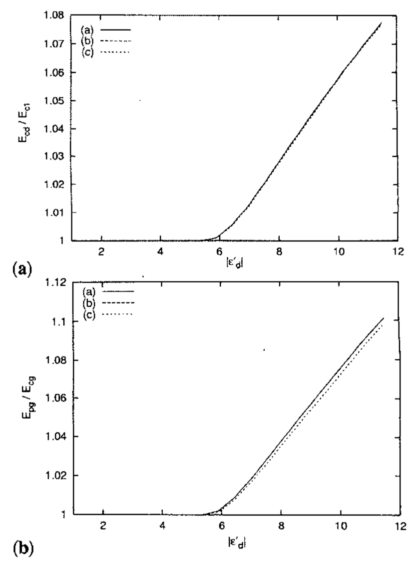

Figure 6. Peak electric field in the arrangements of Figure 2. for ε_d=4 and σ_d=0 to 20 nS/m. (a) 2-dimensional case, (b) Axisymmetrical case.

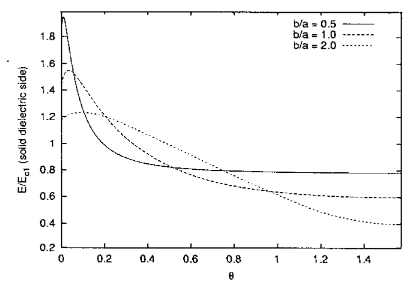

Figure 7. Field distribution in the arrangements of Figure 3 for the 2-dimensional case with ε_d=4 and σ_d=0.

The peak electric field of this arrangement is not at a contact point even when conductivity does not exist in the solid dielectric. It is noted that the distance between the contact point and the point of the peak electric field increases with higher b/a.

Figure 7 also shows that increasing the ratio b/a greatly reduces the peak electric field.

Figure 8 presents the contact-point electric field strength E_{cd} normalized by E_{c1} when no conductivity exists. The constant k in Equation (6) determined for each b/a is compared with the numerical result in Figure 8.

The effect of volume conductivity in the solid dielectric is presented in Figure 9, which shows the ratio E_{pg}/E_{cg} and E_{pg}/E_{c1} in the solid dielectric side. The comparison of Figure 9(a) with Figure 6(b) indicates that the peak E_{pg} is higher than E_{cg}, even when no conductivity exists, and that the presence of conductivity significantly promotes this characteristic, thus increasing E_{pg}/E_{cg} for $|\varepsilon'_d|$>4. This means that in the case of surface contact, the effect of conductivity is much more severe on E_{pg} than on E_{cg}.

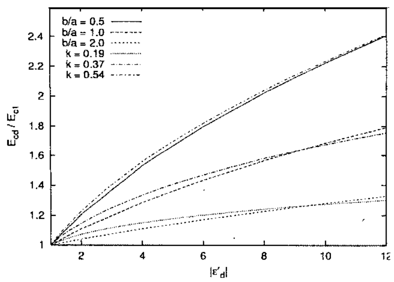

Figure 8. Contact-point electric field in the arrangements of Figure 3 for the 2-dimensional case with ε_d=1 to 12 and σ_d=0.

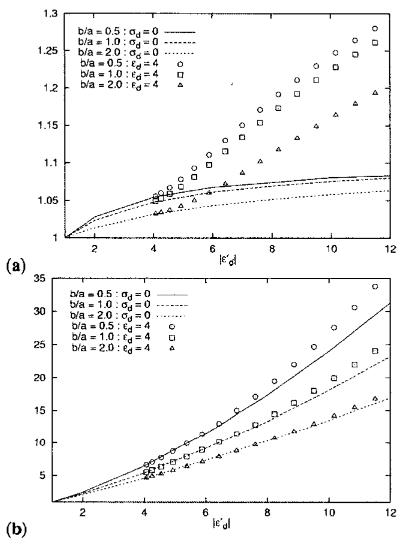

Figure 9. Peak electric field in the arrangements of Figure 3 for the 2-dimensional case. (a) E_{pg}/E_{cg}, (b) E_{pg}/E_{c1}.

On the other hand, Figure 9(b) shows that for the same value of $|\varepsilon'_d|$, the presence of conductivity only slightly increases E_{pg}/E_{c1} (the peak field strength normalized by the contact-point field strength for $\varepsilon'_d = \varepsilon_g$) compared with the value for no conductivity. Further comparison of E_{pg}/E_{c1} is made between line contact and surface contact when ε_d=4, respectively, for arrangement 2(b) and arrangement 3 (b/a=1.0) in Figure 10. E_{pg}/E_{c1} is higher by $\sim$ 20% for arrangement 2(b) of line contact than for arrangement 3 of surface contact.

5 CONCLUSIONS

The effect of the volume conductivity in the solid dielectric has been investigated analytically and numerically on the field behavior in various arrangements with a zero-angle contact condition. The contact conditions consist of point, line, and surface contact.

The electric field behavior or intensification near a contact point principally depends on the absolute value of the complex relative permittivity $|\varepsilon'_d| = |\varepsilon_d - i\sigma_d/\omega\varepsilon_0|$. The peak electric field E_{pd} or E_{pg} increases with $|\varepsilon'_d|$, and volume conductivity usually promotes the field intensification.

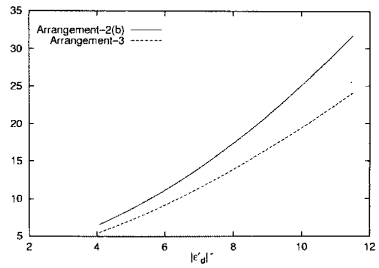

Figure 10. Comparison of peak electric field E_{pg}/E_{c1} between arrangement 2(b) and arrangement 3 (b/a=1.0), for the 2-dimensional case with ε_d=4 and σ_d=0 to 20 nS/m.

In the arrangements of point contact or line contact, the peak electric field does not take place at a contact point when the volume conductivity is higher than a certain value.

In an arrangement of surface contact, the peak electric field usually takes place at a place more or less remote from the contact point, even when no conductivity exists.

The normalized peak value E_{pg}/E_{c1} is higher for line contact than for surface contact.

The peak electric field is considered to become infinite in all arrangements when σ_d becomes infinitely high.

These results give practically useful information to the insulation characteristics, in particular, in the low frequency range, down to dc.

REFERENCES

[1] J. Meixner, "The behavior of electromagnetic fields at edges", Inst. Math. Sci. Res. Report, EM-22, New York University, New York, 1954.

[2] R. Mittra and S. W. Lee *Analytical techniques in the theory of guided waves*, Macmillan, New York, pp. 4–11, 1971.

[3] T. Takuma, T. Kouno and H. Matsuda, "Field behavior near singular points in composite dielectric arrangements", IEEE Trans. Elect. Insul., Vol. 13, pp. 426–435, 1978.

[4] T. Takuma, T. Kawamoto and H. Fujinami, "Effect on conduction on field behavior near singular points in composite medium arrangements", IEEE Trans. Elect. Insul., Vol. 17, pp. 269–275, 1982.

[5] T. Takuma, "Field behavior at a triple junction in composite dielectric arrangements", IEEE Trans. Elect. Insul., Vol. 26, pp. 500–509, 1991.

[6] T. Takuma and T. Kawamoto, "Field intensification near various points of contact with a zero contact angle between a solid dielectric and an electrode", IEEE Trans. PAS., Vol. 103, pp. 2486–2494, 1984.

[7] T. Takuma and T. Kawamoto, "Electric field at various points of contact between rounded dielectric and electrode", 5th ISH, No. 33.09, 1987.

[8] C. A. Brebbia, J. C. F. Telles and L. C. Wrobel, *Boundary element techniques : theory and applications in engineering*, Springer-Verlag, 1984.

[9] C. A. Brebbia, *The Boundary Element Method for Engineers*, Pentech Press, 1984.

[10] K. Hayami and C. A. Brebbia, *A New Coordinate Transformation Method for Singular and Nearly Singular Integrals over General Curved Boundary Element*, Boundary Elements IX, pp. 375–399, 1987.

[11] K. Hayami and C. A. Brebbia, *Quadrature Methods for Singular and Nearly Singular Integrals in 3-D Boundary Element Method*, Boundary Elements X, pp. 238–264, 1988.

[12] K. Hayami, *A Robust Numerical Integration Method for Three-Dimensional Boundary Element Analysis*, Boundary Elements XII, pp. 33–51, 1990.

[13] K. Hayami, "High Precision Numerical Integration Methods for 3-D Boundary Element Analysis", IEEE Transactions on Magnetics, Vol. 26, no. 2, pp. 603–605, 1990.

Manuscript was received on 13 November 2000, in revised form 5 January 2001.